Research Paper

# Analyses of the fatty acid separation principle using liquid chromatography-mass spectrometry

Shigeo Takashima*, Kayoko Toyoshi, Nobuyuki Shimozawa

Division of Genomics Research, Life Science Research Center, Gifu University

**Abstract** Fatty acids vary in their hydrocarbon chain length and the number and position of the double bonds. In this study, we investigated the principle of the separation of fatty acids by reverse-phase liquid chromatography coupled with negative electrospray ionization mass spectrometry (LC-negative ESI-MS). In particular, we aimed to detect very-long-chain fatty acids (VLCFAs) and to distinguish between isomeric unsaturated fatty acids differing in their double bond positions. We found that both saturated and unsaturated fatty acids are not separated by regular chromatography but instead separated by sequential detachment from the column's stationary phase, according to the strength of the organic mobile phase. The interaction of the fatty acids with the stationary phase during chromatographic migration had a minor effect on their separation. Unsaturated fatty acid isomers with different double bond positions were found to be separable, and their elution order was determined by the position of the double bonds relative to the omega carbon. We also found that fibroblasts from the patients with peroxisomal disease show characteristic distribution patterns for some fatty acid isomers in the proposed separation method. Our method is, thus, useful for analyzing a wide range of fatty acid species, including VLCFAs and unsaturated fatty acid isomers, to understand the physiological changes in fatty acid metabolism from clinical samples.

**Key words:** fatty acid, very-long-chain fatty acid, separation principle, liquid chromatography-mass spectrometry, peroxisomal disease

## Introduction

Fatty acids are essential components of living organisms. They form the structure of the cellular membrane, act as signaling molecules (for example, eicosanoids and lysolipids), and serve as cellular energy sources. Fatty acids are classified by multiple chemical characteristics, such as the hydrocarbon chain length, the number of double bonds, and the position of the double bonds. In humans, fatty acids with a chain length of 16 to 22 carbon atoms are the most common[1,2]. In some organs such as the brain and the retina, very-long-chain fatty acids (VLCFAs; fatty acids with 22 or more carbon atom) with carbon numbers of up to 32 and longer exist[3–5]. Moreover, patients with specific types of peroxisomal diseases, a group of diseases caused by dysfunctional metabolic organelles, the peroxisomes, accumulate VLCFAs in their tissues[6,7]. There are no double bonds in saturated fatty acids (SFAs), one or two in monounsaturated fatty acids (MUFAs) or diunsaturated fatty acids (DUFAs), respectively, and more in polyunsaturated fatty acids (PUFAs). Unsaturated fatty acids are further classified by the first double bond position counted from the terminal methyl group (omega carbon), for example, $\omega$-3, $\omega$-6, and $\omega$-9. Distinguished by such chemical features, fatty acids diverge into a number of species, and their physiological functions vary with their chemical characteristics.

To identify fatty acid species in biological samples, gas chromatography-mass spectrometry (GC-MS) and liquid chromatography-mass spectrometry (LC-MS) are commonly used. In a GC-MS assay, fatty acids in biological

*Corresponding author
Shigeo Takashima
Division of Genomics Research, Life Science Research Center, Gifu University, 1−1 Yanagido, Gifu, Gifu 501−1193, Japan
Tel: 058−293−3174, Fax: 058−293−3172
E-mail: staka@gifu-u.ac.jp
Received November 27, 2017. Accepted January 18, 2018.
Epub April 20, 2018.
DOI: 10.24508/mms.2018.06.002

samples are extracted from lipids by hydrolysis and methyl-esterified for better detection[8]. GC-MS requires the vaporization of analytical samples, so it is reliable and applicable for volatile short- to long-chain fatty acids; however, the application of GC-MS to VLCFAs, especially saturated ones, is limited by their poor vaporization capacity and detectability[9,10]. The double bond position is also identifiable with GC-MS. For this purpose, unsaturated fatty acids are derivatized with dimethyl disulfide or pyrrolidine, ionized, and fragmented by electron ionization; then, the double bond position is determined from the characteristic MS spectra. LC-MS complements GC-MS for fatty acid analysis. The extracted fatty acids are analyzed without modification or often derivatized in LC-MS assay[11–13]. For lipidomic analysis, lipids are directly examined, and the constituent fatty acids are identified by the collision-induced dissociation (CID)-mediated lipid fragmentation[2,14]. Although LC-MS can distinguish different fatty acid species according to the chain length and the double bond number, the determination of the double bond position is still challenging. A method that is applicable to a wide range of fatty acid species and distinguishes the chemical specificities would be useful to understand the entire range of fatty acids in biological samples.

Previously, we reported a method for analyzing a series of fatty acids and related molecules in human fibroblast and serum samples[10]. In the previous report, a reverse phase LC conjugated with a negative electrospray ionization-MS (LC-negative ESI-MS) was used, and fatty acids with chain length ranging from 14 (C14) to 44 carbons (C44) with a double bond number of up to 13 (e.g., C44:13) were detected. This method is ideal for analyzing VLCFAs because the ionization efficiency is higher for VLCFAs than for shorter fatty acids. In this study, we investigated the separation principle for the fatty acids on reverse-phase LC by comparing several types of LC columns and expanded the application of the technique to distinguish the double bond positions in the unsaturated fatty acids.

## Materials and Methods

### *Reagents*

The following fatty acid standards and other chemical reagents were used in this study: tetradecanoic acid (C14:0, common name: myristic acid; Sigma-Aldrich, St. Louis, MO; #70079), hexadecanoic acid (C16:0, palmitic acid; Sigma-Aldrich, #76119), octadecanoic acid (C18:0, stearic acid; Sigma-Aldrich, #85679), nonadecanoic acid (C19:0, nonadecylic acid; Sigma-Aldrich, #72332), eicosanoic acid (C20:0, arachidic acid; Sigma-Aldrich, #A-3631), docosanoic acid (C22:0, behenic acid; Tokyo Chemical Industry/TCI, Tokyo, Japan, #B1747), tetracosanoic acid (C24:0, lignoceric acid; TCI, #T0076), pentacosanoic acid (C25:0, pentacosylic acid; TCI, #P0882), hexacosanoic acid (C26:0, cerotic acid; TCI, #C0829), octacosanoic acid (C28:0, montanic acid; Sigma, #284432), *cis*-2-hexadecenoic acid (C16:1 $\omega$-14; TCI, #H0428), *cis*-6-hexadecenoic acid (C16:1 $\omega$-10, sapienic acid; Abcam, Cambridge, United Kingdom, #ab143911), *cis*-9-hexadecenoic acid (C16:1 $\omega$-7, palmitoleic acid; Cayman Chemical, Ann Arbor, MI, USA, #10009871), *cis*-6-octadecenoic acid (C18:1 $\omega$-12, petroselinic acid; Sigma-Aldrich, #P8750), *cis*-9-octadecenoic acid (C18:1 $\omega$-9, oleic acid; Cayman Chemical, # 90260), *cis*-11-octadecenoic acid (C18:1 $\omega$-7, *cis*-vaccenic acid; Matreya LLC, State College, PA, USA, #1266), *cis*,*cis*,*cis*-9,12,15-octadecatrienoic acid (C18:3 $\omega$-3, $\alpha$-linolenic acid; Cayman Chemical, #90210), *cis*,*cis*,-*cis*-6,9,12-octadecatrienoic acid (C18:3 $\omega$-6, $\gamma$-linolenic acid; Cayman Chemical, #90220), *cis*,*cis*,*cis*-5,11,14-eicosatrienoic acid (20:3 $\omega$-6, sciadonic acid; Cayman Chemical, #10009999), *cis*,*cis*,*cis*-8,11,14-eicosatrienoic acid (20:3 $\omega$-6, dihomo-$\gamma$-linolenic acid; Cayman Chemical, #90230), high-performance liquid chromatography (HPLC) grade *tert*-butyl methyl ether (*t*-BME, Sigma-Aldrich, #34875), HPLC grade acetonitrile (Wako, Osaka, Japan, #019-08631), HPLC grade acetone (Wako, #014-08681), HPLC grade 1 mM ammonium acetate (Wako, #018-21041), and 10% ammonia solution (Wako, #013-17505). The fatty acid compounds were dissolved with two volumes of chloroform and one volume of methanol containing 0.05% 2,6-di-*t*-butyl-*p*-cresol (butylated hydroxytoluene, BHT; Nacalai Tesque, Kyoto, Japan, #11421-92) and stored at −20°C until use.

### *Liquid chromatography-mass spectrometry*

For all analyses, we used a Waters Acquity ultra-performance liquid chromatography (UPLC) system, which was equipped with an autosampler/injector and XevoQTof mass spectrometer. For LC, aqueous mobile phase A was purified water containing 1 mM (0.0077% w/v) ammonium acetate and 5.78 mM (0.01% w/v) ammonia. The organic mobile phase B was acetonitrile. Linear gradient conditions with ascending mobile phase B were applied, as shown in Sup-

plementary Fig. S1. The flow rate was set to 0.4 mL/min or 0.2 mL/min, and the column temperature was maintained at 40°C. The injection volume was 5 μL. After LC, the analytes were ionized by negative-ion electrospray ionization (negative ESI) and mass spectra were obtained by the time-of-flight MS. The scan range was set to 100−1000 *m/z*. The setting for the MS system was as follows: capillary voltage, 1.0 kV; sampling cone, 56 (arbitrary value); extraction cone, 4.0 (arbitrary value); source temperature, 125°C; desolvation temperature, 350°C; cone gas flow, 60 L/h; and desolvation gas flow, 1000 L/h. The data were analyzed by Masslynx and Quanlynx software (Waters) and graphs were prepared by Microsoft Excel. ACD ChemSketch was used to draw chemical structural formula.

*LC columns*

The following columns (Waters Acquity UPLC columns) were used: BEH (Ethylene Bridged Hybrid) C18 (2.1×100 mm, particle size 1.7 μm, pore size 130 Å, #186002352), BEH C8 (2.1×50 mm, particle size 1.7 μm, pore size 130 Å, #186002877), Protein BEH C4 (2.1×50 mm, particle size 1.7 μm, pore size 300 Å, #186004495, and 2.1×100 mm, particle size 1.7 μm, pore size 300 Å, #186004496), BEH C18 VanGuard Pre-Column (2.1×5 mm, particle size 1.7 μm, pore size 130 Å, #186003975), BEH C8 VanGuard Pre-Column (2.1×5 mm, particle size 1.7 μm, pore size 130 Å, #186003978), and Protein BEH C4 VanGuard Pre-Column (2.1×5 mm, particle size 1.7 μm, pore size 300 Å, #186004623).

*Fatty acid purification from fibroblasts*

A neonatal human skin fibroblast line (NB1RGB, #RCB0222) was obtained from RIKEN BRC through the National Bio-Resource Project (NBRP) of the Ministry of Education, Culture, Sports, Science, and Technology (MEXT), Japan. An adult skin fibroblast line (contY) was established by us from a healthy adult male[15]. Written informed consent was obtained from the donner. A neonatal skin fibroblast line (F-12) was also established from a biopsy sample obtained from a peroxisome biogenesis disorder (PBD) patient carrying *PEX2* mutation, who was diagnosed with Zellweger syndrome[10]. Written informed consent was obtained from the patient's parents. The purification of total fatty acids from fibroblasts was performed as described previously[10]. Briefly, a pellet of approximately $1\times10^6$ cells was mixed with 400 μL of acetonitrile and 50 μL of 5 M hydrochloric acid in a glass tube and lysed by vigorous vortexing for 1 min. The cell lysate was incubated at 100°C in an oil bath for 1 h. After bringing the lysate to room temperature, 800 μL of *t*-butyl methyl ether (*t*-BME), 100 μL of methanol containing C19:0 (as an internal standard; 1 μg/mL), and 400 μL of purified water were added, and the sample was vortexed again for 1 min. After centrifugation at 200×*g* for 5 min, the upper phase was collected, 800 μL of water was added, and the sample was vortexed again. After phase separation by 5 min centrifugation, the upper organic phase (*t*-BME) containing fatty acids was collected in a glass sample vial with a polytetrafluoroethylene (PTFE)-lined cap (GL Sciences, Tokyo, Japan, #1030−51023 and #1030-45260). The organic solvent was evaporated under a stream of nitrogen gas. The fatty acids were reconstituted in 100 μL of acetone and used for LC-MS analysis.

*Double bond nomenclature of fatty acids*

In this paper, the position of the double bond from the terminal methyl group (omega carbon) is denoted by omega (ω) numbers so that ω-3 or ω-9 indicates the position of the first double bond between the 3rd and 4th carbons (ω-3) or 9th and 10th carbons (ω-9), respectively. In some specific cases, we use the *cis*-x nomenclature, such as *cis*-12 or *cis*-15, in which the double bond position is counted from the anti-terminal carboxyl group to clarify that the double bond is in the *cis* conformation rather than *trans* conformation as appears in the chemical formula.

This study was approved by the Ethical Committee of the Graduate School of Medicine, Gifu University (permission number: 29-286).

## Results

*Mobile phase strength-dependent detachment behavior of fatty acids from the LC column: The fatty acid separation principle*

We previously reported a method for the analysis of a range of fatty acids found in biological samples[10]. The total fatty acid species including saturated and unsaturated fatty acids, as well as very-long-chain fatty acids (VLCFAs) found in peroxisomal disease patients, were analyzed in a single assay. In the present study, we modified our method, aiming for improved detection of VLCFAs and the precise separation of unsaturated fatty acids according to the num-

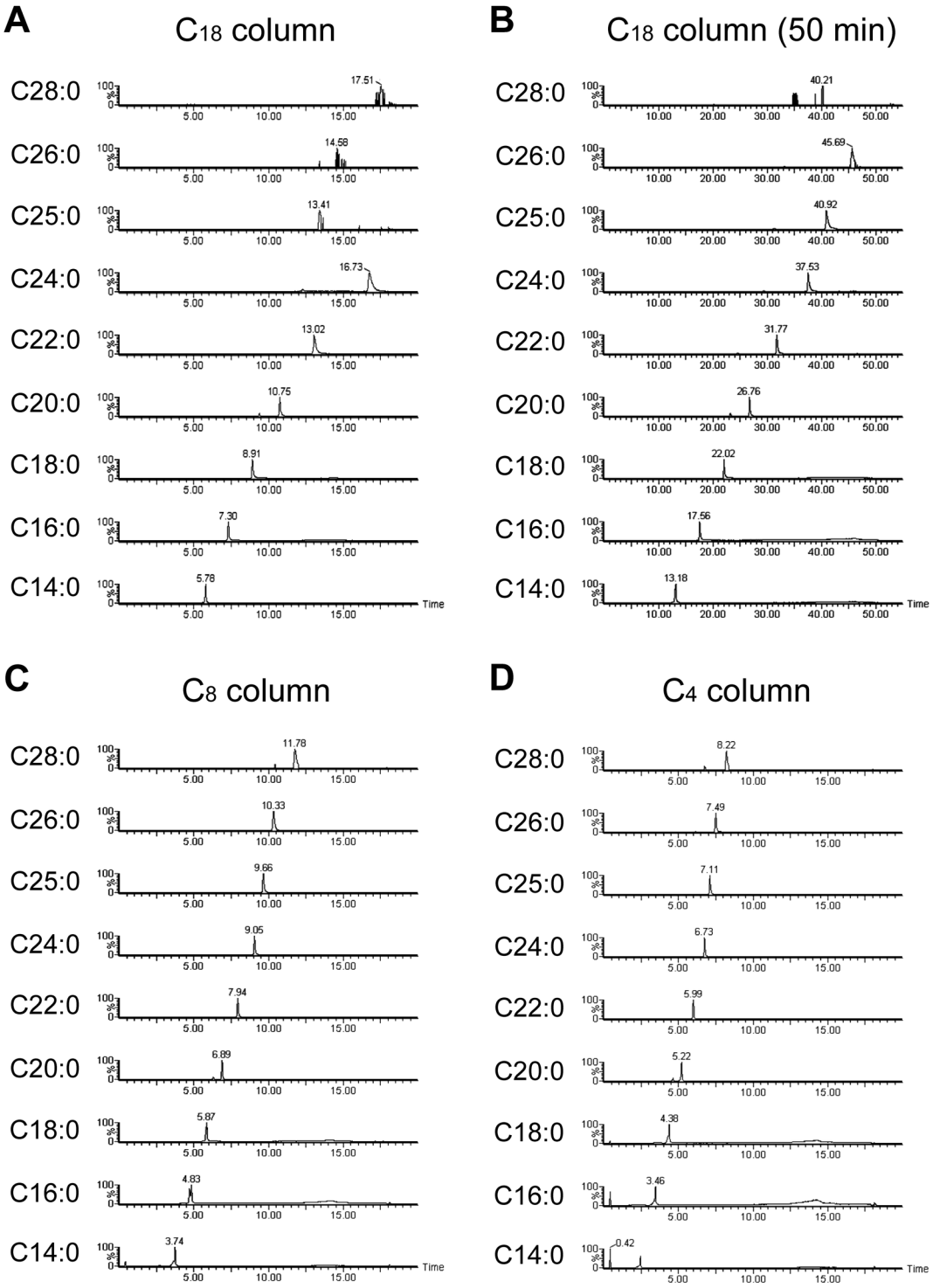


**Fig. 1. Comparison of LC columns with different stationary phases upon fatty acid analysis.**
(A−D) A fatty acid standard mixture (C14:0, C16:0, C18:0, C20:0, C22:0, C24:0, C25:0, C26:0, and C28:0) was separated with $C_{18}$ (A and B), $C_8$ (C), or $C_4$ (D) columns. A 15-min linear gradient was used except for (B), where a 50-min gradient was used. Mass chromatograms of the fatty acid species are shown. The ***x***-axis indicates the retention time and the ***y***-axis indicates the relative intensity. (E, F) Comparison between LC columns. The ***x***-axes indicate the number of carbons, and the ***y***-axes indicate the retention time in (E) or % B in (F). Trend lines are shown as black lines in (F). (G) Comparison of the column length. Five-centimeter (cm) and 10-cm $C_4$ columns are compared. The retention time for each fatty acid species is normalized by the retention time of C14:0, and the time difference against C14:0 ($\Delta RT_{C14:0}$) is shown.

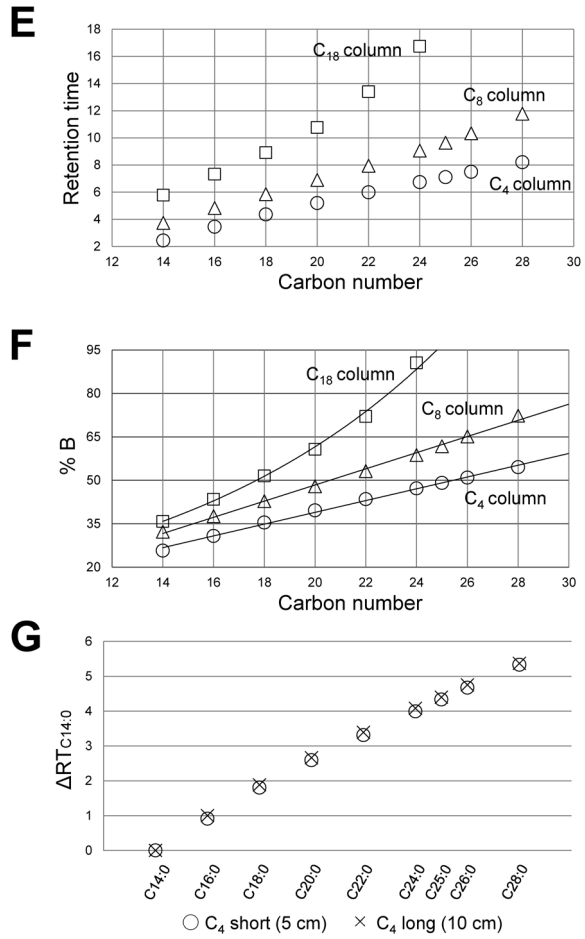


**Fig. 1. Continued.**

ber and position of the double bond(s). We evaluated three types of LC columns with different stationary phases: $C_{18}$, $C_8$, and $C_4$ (see Materials and Methods for details), where $C_{18}$ has the highest hydrophobicity and $C_4$ has the lowest. A saturated fatty acid standard mixtures ranging from C14 to C28 (1 $\mu$g/mL of C14:0, C16:0, C18:0, C20:0, and C22:0, and 0.1 $\mu$g/mL of C24:0, C25:0, C26:0, and C28:0) were analyzed using the three columns with a gradient LC (LC condition 1: 0.4 mL/min flow rate, 15 min linear gradient from 20% B to 95% B followed by 2.5 min static 95% B; see Supplementary Fig. S1). With the $C_{18}$ column, the fatty acids eluted from shorter ones at constant time intervals, but, VLCFAs such as C25:0 and longer failed to elute within the assay time (Fig. 1A). When the gradient time was extended to 50 min (LC condition 2; Fig. 1B) or the organic phase was kept at 95% for 2 h after the LC gradient (LC condition 3; data not shown), the VLCFAs failed to elute or eluted with broad peaks, respectively, indicating the intense adhesion of the VLCFAs to the $C_{18}$ stationary phase. Thus, we conclude that the $C_{18}$ stationary phase is not suitable for analyzing saturated VLCFAs.

For the $C_8$ column, the fatty acids eluted earlier than with the $C_{18}$ column (Fig. 1C), and all standard fatty acid molecules including VLCFAs were successfully eluted. For the $C_4$ column, all fatty acids eluted much earlier (Fig. 1D). We assessed the correlation between fatty acid length and retention time (Fig. 1E). The $C_4$ and $C_8$ columns had a high correlation coefficient ($r$=0.9985 for $C_4$, and $r$=0.9982 for $C_8$) with a linear trend line, whereas the $C_{18}$ columns had a low correlation coefficient ($r$=0.9864; calculated from the data of C14:0 to C24:0). This indicates that $C_4$ and $C_8$ columns are suitable for separating a long-range fatty acid mixture, including VLCFAs.

To understand the relationship between the fatty acids, stationary phases, and the organic mobile phase in more detail, we plotted the detachment time of the fatty acids (calculated from the column hold-up time and the fatty acid retention time) and the strength of the organic mobile phase (% B, acetonitrile) at the detachment time. With $C_{18}$ columns, the best-fit trend line on the plot was exponential (Fig. 1F), and the function of the trend line is given by

$$\%B = 10.106\, e^{0.0904\ lenFA},$$

where *lenFA* indicates the carbon chain length of the saturated fatty acid. We estimated the longest fatty acid detectable with the $C_{18}$ column using this function when the maximum mobile phase B was 95%. The estimated longest fatty acid was C24:0, which is consistent with the above observation that C25:0 and longer fatty acids failed to elute from the $C_{18}$ column. The best-fit trend line became linear when the data up to C22:0 was used (data not shown). These data confirmed that the $C_{18}$ column does not fit the VLCFA analysis. For the $C_8$ column, the trend line was linear (Fig. 1F):

$$\%B = 2.7925\ lenFA - 7.483,$$

and C36:0 is estimated to be the longest detectable fatty acid if this trend continues. We previously reported the detection of C34:0 in human plasma and fibroblast samples using a $C_8$ column, although C36:0 has not been detected[10]. With the $C_4$ column, the trend line was also linear (Fig. 1F):

$$\%B = 2.0341\ lenFA - 1.7692,$$

and the estimated longest fatty acid was C47:0, although the existence of C47:0 is unlikely in biological samples. Overall, the above observations indicate that each column

has a specific limit in the length of detectable saturated fatty acids.

Next, we examined the effect of the column length. Five-centimeter (cm) and 10-cm columns with the $C_4$ stationary phase were compared. With the 5-cm $C_4$ column, C14:0 eluted at 1.61 min with a 0.4-mL/min flow rate and C28:0 eluted at 6.94 min. Thus, the time difference between C14:0 and C28:0 is 5.33 min. With the 10-cm $C_4$ column, C14:0 eluted at 2.81 min and C28:0 at 8.18 min. The time difference between C14:0 and C28:0 is 5.37 min, which is comparable to the case of the 5-cm column. To compensate for the difference in the hold-up time between the two columns, the retention time of C14:0 was used as a reference. The adjusted retention times of the standard fatty acids became almost identical between the 5-cm and 10-cm columns (Fig. 1G), indicating that lengthening the column

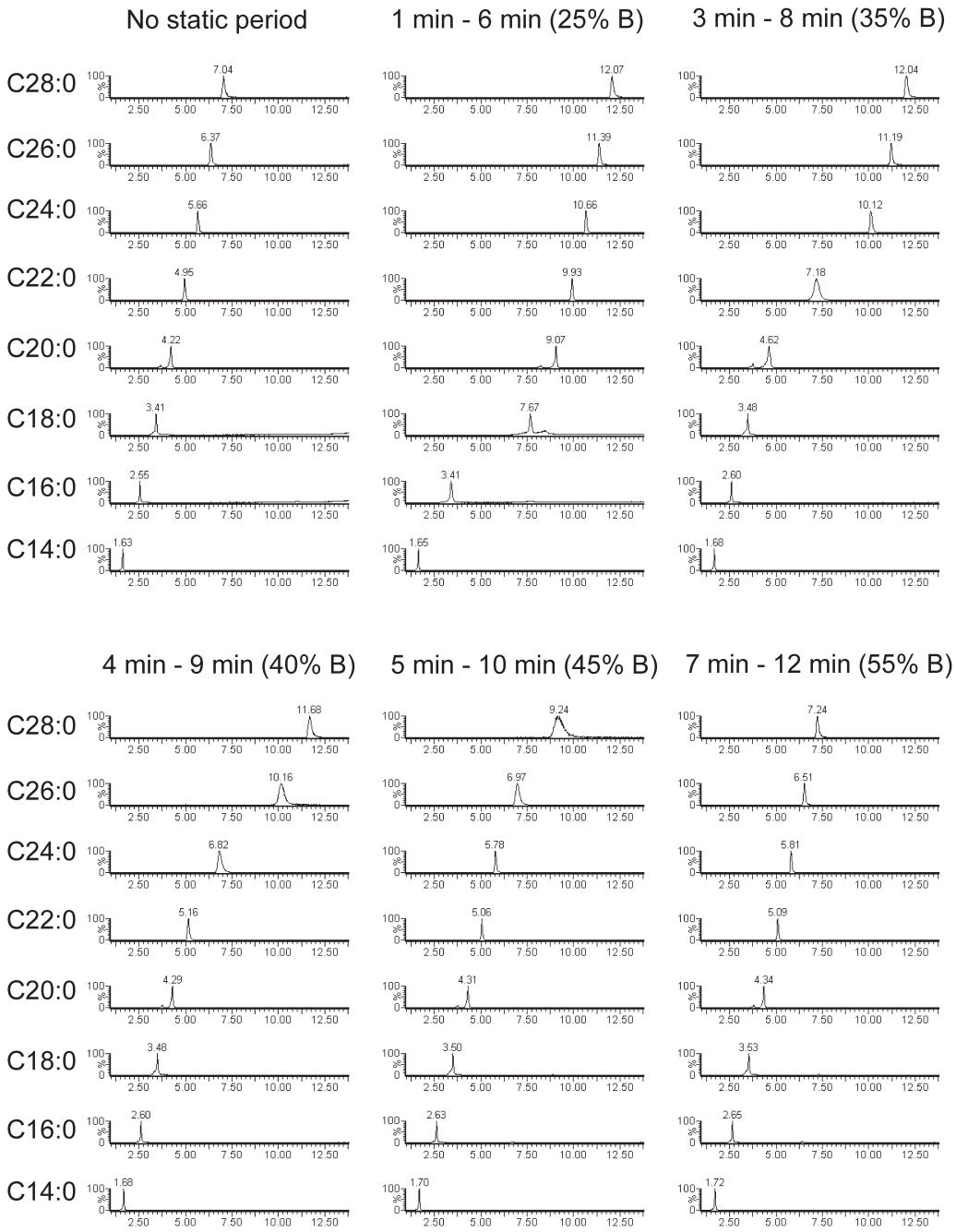


**Fig. 2. The static phase in the LC gradient affects the migration of specific fatty acid species.**
Fatty acid standards were separated by the LC conditions with a 5-min static phase, as shown in Supplementary Fig. S1. The ***x***-axis indicates the retention time and the ***y***-axis indicates the relative intensity. The migration of some fatty acid species is affected by each LC condition.

does not improve the separation of fatty acids. From the above results, the retention of the fatty acids seemed to be largely dependent on the concentration of the organic mobile phase (i.e., acetonitrile), and the interactions between the fatty acids and the column-filled stationary phase during chromatographic migration has a minor effect.

As described, the mobile phase strength seemed to determine the timing of the detachment of fatty acids from the stationary phase. Utilizing this rule, we divided the fatty acid standard mixture into portions by inserting a 5-min static period in the LC gradient at several time points, as indicated in Fig. 2 (LC conditions 3 to 8; $C_4$ column was used). For the first condition, the gradient paused after 1 min of analytical time, when the mobile phase B was 25%, until 6 min; then, the gradient was resumed. Under this condition, C14:0 eluted normally, whereas C16:0 and C18:0 were trapped in the static phase; thus, their migration slowed. C20:0 and longer fatty acids eluted with a 5-min delay but in the same proportion as under the continuous gradient condition. When the gradient was paused at 3 min (35%B; LC condition 5), C14:0 to C18:0 had eluted already, the migration of C20:0 to C24:0 slowed, and C26:0 and C28:0 were proportionally delayed by 5 min. All of the standard fatty acids eluted by 7 min (55%B), indicating that fatty acids up to C28:0 had detached from the $C_4$ stationary phase before the concentration of mobile phase B reached 55%, which is also predicted by the above formula. This simple separation principle for fatty acids enables the fractioning of fatty acid mixtures, which is also shown below.

### *Separation of unsaturated fatty acids with double bond numbers*

Next, we examined unsaturated fatty acids to see if they behave in the same manner as the SFAs in biological samples. Total fatty acids were extracted from human fibroblasts (NB1RGB) and analyzed with the $C_8$ column. As in our previous report, unsaturated fatty acids showed a regular elution pattern[10] (Fig. 3A; Supplementary Fig. S2). Among fatty acids with the same hydrocarbon chain length, the one with more double bonds eluted earlier than the ones with less double bonds. For example, among the C20 fatty acids, the elution order is C20:5, C20:4, C20:3, C20:2, and C20:1, and C20:0 elutes last. We examined the relationship of hydrocarbon chain length and retention time for MUFAs, DUFAs, and PUFAs with three and four double bonds (tri-unsaturated and tetra-unsaturated fatty acids, respectively) and found a linear correlation (Fig. 3B). The unsaturated fatty acids show constant and predictable elution pattern, as in the case of SFAs.

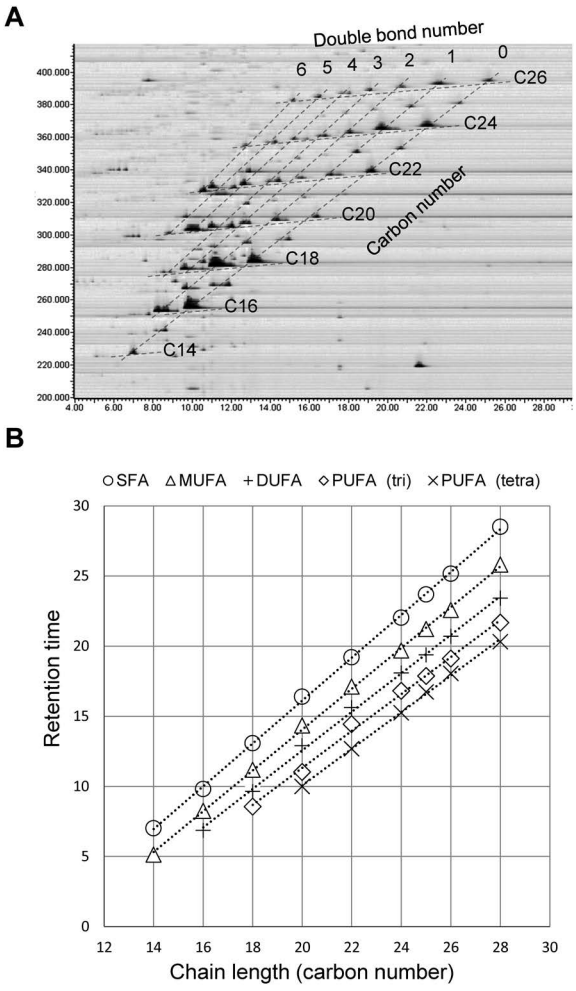


**Fig. 3. Correlation between the retention time and the hydrocarbon chain length of unsaturated fatty acids.** (A) A 2-D map analysis of the fatty acids. Fatty acids from control human fibroblasts (NB1RGB) analyzed with the $C_8$ column. The ***x***-axis represents the retention time and the ***y***-axis represents ***m***/***z***. The fatty acid species are shown on the map as black spots. The carbon number and the double bond number in the fatty acids are annotated in the panel (the same panel without annotations is shown in Supplementary Fig. S2). (B) Retention times of MUFAs (C14:1 to C28:1), DUFAs (C16:2 to C28:2), and PUFAs with three double bonds (tri-unsaturated fatty acids; C18:3 to C28:3) and four double bonds (tetra-unsaturated fatty acids; C20:4 to C28:4), as well as SFAs (C14:0 to C28:0), are plotted on the graph. All show linear correlations.

To separate the fatty acid species from the biological samples, we improved the separation method by modifying the LC gradient. We inserted a 5-min decrease in the organic phase (LC condition 9) rather than inserting a static

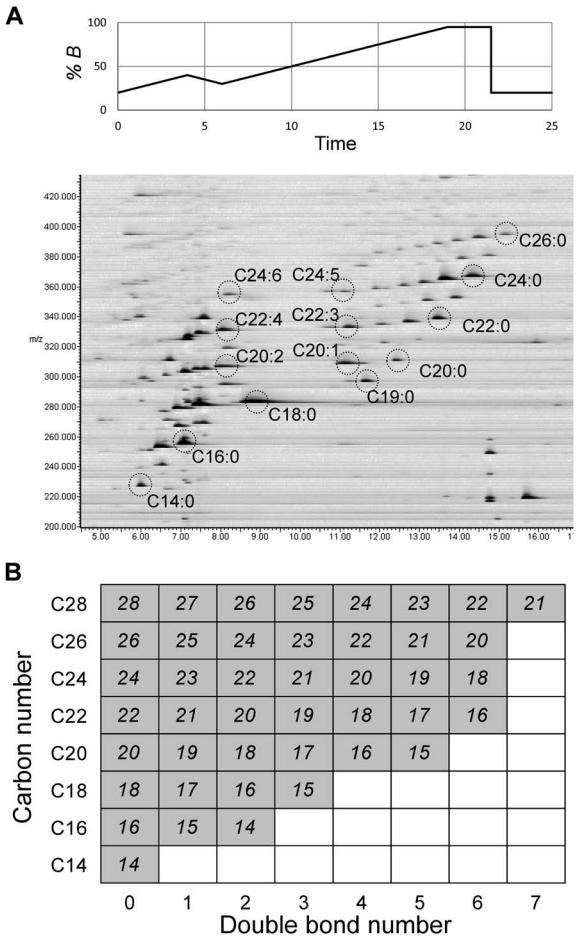


**Fig. 4. Separation of biological fatty acids into fractions.** (A) Fatty acids from control fibroblasts (contY) were analyzed with a modified gradient LC (LC condition 9; upper graph) with a $C_4$ column and are shown in a 2-D map (lower panel). Fatty acids are divided into two portions, one with elution index (EI) 18 and below and the other with EI 19 and above. Saturated fatty acids and selected unsaturated fatty acids at the separation border are labeled. (B) An EI chart of fatty acids. The EI values of even-numbered fatty acids detected in control human fibroblasts (C14 to C28) are shown.

phase as described above. Using this modification, we were able to clearly separate the biological fatty acids into fractions (Fig. 4A). The separation was very clear according to the elution index, which shows total hydrophobicity of the given fatty acid species (Fig. 4B; see Discussions for more detail). Using this method, fatty acid mixtures can be separated into fractions divided by their hydrophobicity.

### *Separation of unsaturated fatty acids according to the position of the double bonds*

As shown above, a number of unsaturated fatty acids including MUFAs, DUFAs, and PUFAs, are detectable in human tissue samples. Moreover, very-long-chain polyunsaturated fatty acids (VLC-PUFAs) are elevated in peroxisomal diseases[2,10,14]. All can be separated by LC according to the chain length and double bond numbers. Because the unsaturated fatty acids are also distinguished by their double bond positions, we further separated unsaturated fatty acids according to their double bond positions.

To determine the basic rule concerning double-bond-position-dependent fatty acid separation, we compared standard unsaturated fatty acids on LC with the 50-min gradient (LC condition 2). First, we used three octadecenoic acids (C18:1) with different double bond positions such as at $\omega$-9 position (oleic acid), $\omega$-7 (*cis*-vaccenic acid), and $\omega$-12 (petroselinic acid) (Fig. 5A). Five microliters of 10 $\mu$M solutions were injected and analyzed with the $C_8$ column. Among the three octadecenoic acids, *cis*-vaccenic acid ($\omega$-7) eluted first, oleic acid ($\omega$-9) eluted second, and petroselinic acid ($\omega$-12) eluted last. Three peaks separating a mixture of the octadecenoic acids were also detectable. The double bond position, which is closest to the omega carbon in *cis*-vaccenic acid, farthest in petroselinic acid, and in between in oleic acid, is a possible determinant of the elution order. It seems that as the continuous saturated hydrocarbon chain terminated with a methyl group (containing the omega carbon) becomes longer, the unsaturated fatty acid becomes more hydrophobic, thus prolonging the elution time.

We also analyzed three hexadecenoic acids (C16:1) with double bond positions at $\omega$-7 (palmitoleic acid), $\omega$-10 (sapienic acid), and at $\omega$-14 (*cis*-2-hexadecenoic acid) (Fig. 5B). As indicated by the results for the 18:1 fatty acids, the double bond position relative to the omega carbon correlated to the elution order (thus the elution order was palmitoleic acid, sapienic acid, and *cis*-2-hexadecenoic acid). This confirmed the idea that a double bond closer to the omega carbon makes the MUFAs less hydrophobic; in other words, longer, saturated hydrocarbon chains ending with the omega carbon on the terminal methyl group makes MUFAs more hydrophobic.

To expand this idea to PUFAs, we compared two types of linolenic acid (octadecatrienoic acid, C18:3), $\alpha$-linolenic acid and $\gamma$-linolenic acid. Alpha-linolenic acid possesses three double bonds at the $\omega$-3, 6, and 9 positions, and $\gamma$-linolenic acid has double bonds at the $\omega$-6, 9, and 12 positions (Fig. 5C). The peaks of these two fatty acids were separated

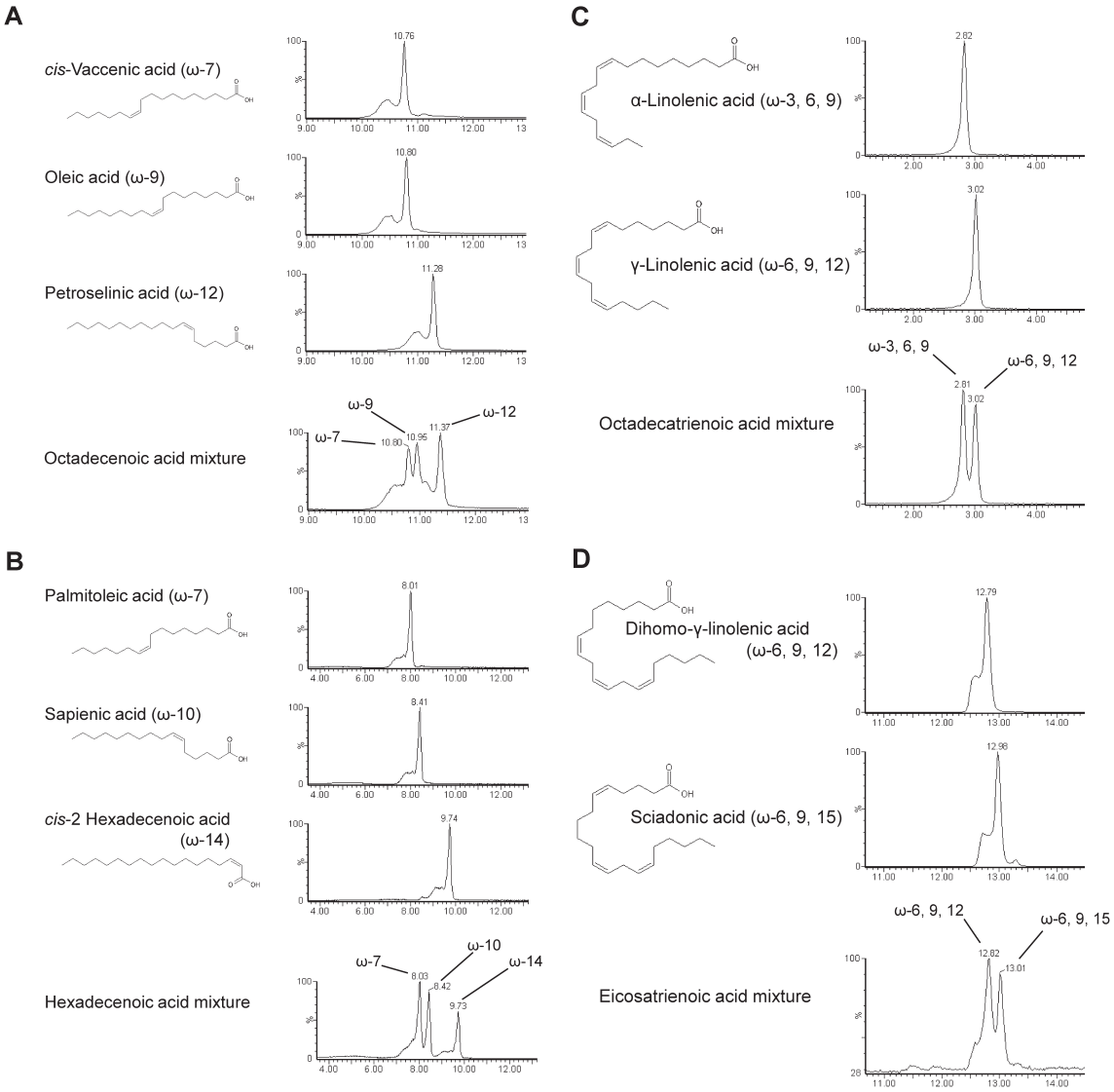


**Fig. 5. Elution order of unsaturated fatty acids.**
(A) Mass chromatogram of three octadecenoic acids (C18:1), ***cis***-vaccenic acid (*ω*-7), oleic acid (*ω*-9), petroselinic acid (*ω*-12), and their mixture are shown. (B) Mass chromatogram of three hexadecenoic acids (C16:1), palmitoleic acid (*ω*-7), sapienic acid (*ω*-10), ***cis***-2 hexadecenoic acid (*ω*-14), and their mixture. (C) Mass chromatogram of two octadecatrienoic acids (18:3), *α*-linolenic acid (*ω*-3, 6, 9), *γ*-linolenic acid (*ω*-6, 9, 12), and their mixture. (D) Mass chromatogram of two eicosatrienoic acids (C20:3), dihomo-*γ*-linolenic acid (*ω*-6, 9, 12), sciadonic acid (*ω*-6, 9, 15), and their mixture.

clearly, and *α*-linolenic acid, which has the first double bond closer to the omega carbon, again, eluted before *γ*-linolenic acid, which has a more distant double bond. Concerning the C18:1 and C16:1 MUFAs, the elution order of the C18:3 PUFAs was found to be determined by the position of the first double bond.

We also examined PUFAs with the same proximal double bond but different distal double bond. Two C20:3 PUFAs (eicosatrienoic acids), dihomo-*γ*-linolenic acid (*ω*-6, 9, and 12) and sciadonic acid (*ω*-6, 9, and 15), were examined (Fig. 5D). These two eicosatrienoic acids have identical proximal and second-proximal double bonds, but the positions of the distal double bond are different. Dihomo-*γ*-linolenic acid eluted before sciadonic acid, thus indicating the non-proximal double bond also affects the elution order. Taken together, the total proximity of the all double bonds to the omega carbon is the determining factor in the elution order of PUFAs.

### *Detailed fatty acid profile of human fibroblasts*

Finally, we compared the fatty acids of human fibroblasts retrieved from a control subject and a patient with peroxi-

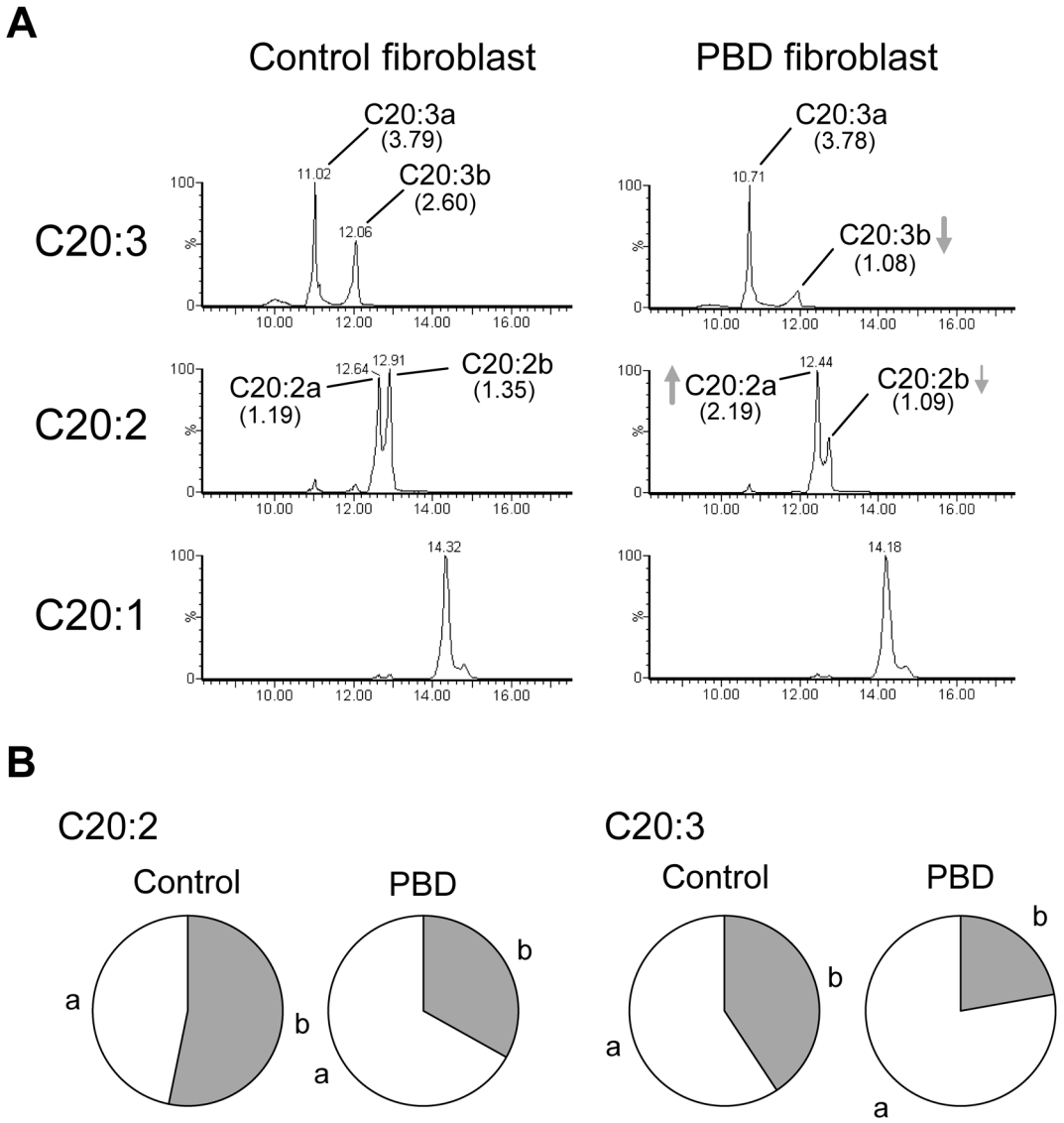


**Fig. 6. Quantitatively changed unsaturated fatty acid isomers found in fibroblasts of peroxisome biogenesis disorder.**
(A) Multiple peaks representing different fatty acid isomers in the C20 lineage (C20:2 and C20:3) are shown. The ***x***-axis indicates the retention time and the ***y***-axis indicates relative intensity. In the PBD fibroblasts, the proportion of each two peaks in C20:2 and C20:3 are altered. The numbers in parentheses indicate the relative amount with respect to C20:0. The arrows indicate an increase or a decrease of each fatty acid isomer. (B) Pie charts representing the proportion of C20:2 isomers or C20:3 isomers in the control and PBD fibroblasts are shown.

some biogenesis disorder (PBD), a type of peroxisomal disease involving defective peroxisomal biosynthesis[6,7]. Fatty acids were extracted from the total lipids by acid hydrolysis and assayed with the $C_8$ column with a 50-min gradient (LC condition 2). We searched for unsaturated fatty acids giving multiple peaks representing double-bond position differences and found several examples (Fig. 6A). Interestingly some of the peaks differ in intensity between the control and PBD fibroblasts. C20:2 had two peaks, and we tentatively identify that which eluted earlier as C20:2a and that which eluted later as C20:2b. We confirmed that they both have the same carbon number by comparing their $^{13}C$ ratios (Supplementary Fig. S3). The amount of C20:2a and C20:2b fatty acids were comparable in the control fibroblasts, whereas the amount of C20:2a was double that of C20:2b in the PBD fibroblasts (Fig. 6B). C20:3 also had two peaks, C20:3a and C20:3b (Fig. 6A, Supplementary Fig. S3). C20:3a was clearly more abundant in the PBD fibroblasts compared to C20:3b (Fig. 6B). The relative quantification against internal C20:0 revealed the nearly two-fold increase or decrease of C20:2a or C20:3b, respectively, in the PBD fibroblasts (Fig. 6A). The separation of fatty acid isomers was, thus, found to be useful to understand the metabolic changes in cellular fatty acids.

## Discussion

*Fatty acids separation principle: Organic phase strength-dependent detachment from LC column*

We investigated the separation principle for fatty acids and found that the separation depends on their detachment behavior from the stationary phase of the LC column, unlike regular chromatography. The fatty acids sequentially detached from the stationary phase along with the organic mobile phase once an appropriate concentration to retrieve each fatty acid species from the stationary phase was achieved. Among the SFAs, longer SFAs elute after shorter SFAs because of their higher hydrophobicity, which increases the adhesion strength to the stationary phase (e.g., C22:0 elutes after C20:0). When SFAs and unsaturated fatty acids are compared, SFAs elute after the MUFAs with the same or longer hydrocarbon chain by one carbon, but elute before MUFAs longer by two hydrocarbons (for example, C22:0 elutes after C22:1 and C23:1 but before C24:1). MUFAs elute after the SFAs shorter by two hydrocarbons, MUFAs shorter by one hydrocarbon, and DUFAs with the same hydrocarbon length (C22:1 elutes after C20:0, C21:1, and C22:2) but elute before MUFAs longer by one hydrocarbon and DUFAs longer by two hydrocarbons (C22:1 elutes before C23:1 and 24:2). These features indicate that acquiring one double bond can compensate for the increased hydrophobicity provided by one hydrocarbon. A simple method to estimate the elution order (or retention time) of given fatty acids is to calculate and compare the elution index (EI). The EI is calculated by deducting the number of double bonds from the number of carbon atoms of a given fatty acid. For example, in the case of C22:3, [total carbon number] 22 − [double bond number] 3=[EI] 19. With the $C_4$ column, a fatty acid elutes before the fatty acids with larger EI, and fatty acids sharing the same EI elute around the same time, aside from the SFAs that elute slightly later than the others. With the $C_8$ column, longer fatty acids elute slightly earlier than the shorter fatty acids when their EI is the same. The EIs of selected human fibroblast fatty acids are shown in Fig. 4B.

*Double bond position-specific fatty acid separation*

We also investigated the elution order of isomeric unsaturated fatty acids that differ from each other by the position of the double bond(s). By examining C16:1 and C18:1 MUFAs, as well as C18:3 and C20:3 PUFAs, we found that the first double bond from the omega carbon is the major determinant of the elution order among the isomers. A double bond closer to the omega carbon makes the unsaturated fatty acid less hydrophobic; thus, it elutes earlier than isomers having the first double bond further from the omega carbon. Moreover, we found that the proximity of other double bonds also affects the elution order. By and large, when the hydrocarbon chain length is identical, fatty acids with more double bonds elute earlier than those with fewer double bonds, and, if the number of the double bonds is the same, those with double bond(s) closer to the omega carbon elute earlier than others. Following these criteria, we found that many isomeric unsaturated fatty acids exist in human fibroblasts and the concentrations of some of these fatty acids change in PBD patients.

We could not identify the exact double bond position of these fatty acids because locating the double bond by ESI-MS is still challenging. Collision-induced dissociation (CID) is often used with ESI-MS to fragment target ions but does not give definitive product ions to determine the position of the double bond(s) of unsaturated fatty acids[16,17]. To overcome this problem, several derivatization methods have been developed[18,19]. The derivatization of the terminal carboxyl group with *N*-(4-aminomethylphenyl) pyridinium (AMPP) enables fatty acids to be detected with more sensitive positive ESI (ESI+), and the CID fragmentation generates product ions for double bond location[18,20]. Zhao et al. recently reported that the epoxidation of unsaturated fatty acids using low temperature plasma followed by CID fragmentation gives product ions generated at the site of epoxidation, and, thus, the double bond position can be determined[19]. A combination of our method with these derivatization methods will further improve our understanding of the entire fatty acid species in biological samples, allowing the hydrocarbon chain length, double bond numbers, and double bond positions to be distinguished.

VLCFAs increase in some human peroxisomal disease patients and are considered pathogenic, although their pathogenicity should be confirmed clinically[6,7]. Relatively few VLCFA species, such as C26:0 and C24:0, are commonly used as diagnostic markers for peroxisomal diseases[6,21], but significantly more VLCFA species accumulate in patients, as we and others have previously reported[2,10,14]. Our current analysis of the patient fibroblasts with distinguishing double bond positions revealed clear fluctuations in additional fatty acid species such as C20:2a and C20:3b, for which we do not know the exact

double bond position. Profiling the entire fatty acid range, distinguishing the double bond position, and identifying the changes in additional fatty acid species in peroxisomal disease patients will give us a new insight of the metabolic changes in patients and reveal the pathology of peroxisomal diseases.

## Acknowledgements

We thank Dr. Tsuneo Imanaka at Hiroshima International University, Dr. Masashi Morita and Dr. Kosuke Kawaguchi at the University of Toyama, and Dr. Kazuaki Yokoyama, Dr. Kotaro Hama, and Dr. Yuko Fujiwara at Teikyo University for their valuable comments. This work was supported by JSPS KAKENHI grant numbers JP25860855 for ST, and 15H048750001, 15K153890001 for NS from the Japan Society for the Promotion of Science, Japan. This work was also supported by research aid funds from the Koshiyama Foundation for the Promotion of Science and Technology, and the Takahashi Industrial and Economic Research Foundation for ST.

## Conflict of Interest

The authors declare no conflicts of interest.

### References

1) Kingsbury KJ, Paul S, Crossley A, Morgan DM: The fatty acid composition of human depot fat. *Biochem J* 78: 541−550, 1961.
2) Abe Y, Honsho M, Nakanishi H, Taguchi R, Fujiki Y: Very-long-chain polyunsaturated fatty acids accumulate in phosphatidylcholine of fibroblasts from patients with Zellweger syndrome and acyl-CoA oxidase1 deficiency. *Biochim Biophys Acta* 1841: 610−619, 2014.
3) Aveldaño MI: A novel group of very long chain polyenoic fatty acids in dipolyunsaturated phosphatidylcholines from vertebrate retina. *J Biol Chem* 262: 1172−1179, 1987.
4) Poulos A, Sharp P, Johnson D, Easton C: The occurrence of polyenoic very long chain fatty acids with greater than 32 carbon atoms in molecular species of phosphatidylcholine in normal and peroxisome-deficient (Zellweger's syndrome) brain. *Biochem J* 253: 645−650, 1988.
5) Agbaga MP, Mandal MN, Anderson RE: Retinal very long-chain PUFAs: New insights from studies on ELOVL4 protein. *J Lipid Res* 51: 1624−1642: 2010.
6) Steinberg SJ, Dodt G, Raymond GV, Braverman NE, Moser AB, Moser HW: Peroxisome biogenesis disorders. *Biochim Biophys Acta* 1763: 1733−1748, 2006.
7) Shimozawa N: Molecular and clinical findings and diagnostic flowchart of peroxisomal diseases. *Brain Dev* 33: 770−776, 2011.
8) Takemoto Y, Suzuki Y, Horibe R, Shimozawa N, Wanders RJ, et al: Gas chromatography/mass spectrometry analysis of very long chain fatty acids, docosahexaenoic acid, phytanic acid and plasmalogen for the screening of peroxisomal disorders. *Brain Dev* 25: 481−487, 2003.
9) Liu A, Chang J, Lin Y, Shen Z, Bernstein PS: Long-chain and very long-chain polyunsaturated fatty acids in ocular aging and age-related macular degeneration. *J Lipid Res* 51: 3217−3229, 2010.
10) Takashima S, Toyoshi K, Itoh T, Kajiwara N, Honda A, et al: Detection of unusual very-long-chain fatty acid and ether lipid derivatives in the fibroblasts and plasma of patients with peroxisomal diseases using liquid chromatography-mass spectrometry. *Mol Genet Metab* 120: 255−268, 2017.
11) Johnson DW: A rapid screening procedure for the diagnosis of peroxisomal disorders: quantification of very long-chain fatty acids, as dimethylaminoethyl esters, in plasma and blood spots, by electrospray tandem mass spectrometry. *J Inherit Metab Dis* 23: 475−486, 2000.
12) Al-Dirbashi OY, Santa T, Rashed MS, Al-Hassnan Z, Shimozawa N, et al: Rapid UPLC-MS/MS method for routine analysis of plasma pristanic, phytanic, and very long chain fatty acid markers of peroxisomal disorders. *J Lipid Res* 49: 1855−1862, 2008.
13) Bromke MA, Hochmuth A, Tohge T, Fernie AR, Giavalisco P, et al: Liquid chromatography high-resolution mass spectrometry for fatty acid profiling. *Plant J* 81: 529−536, 2015.
14) Hama K, Nagai T, Nishizawa C, Ikeda K, Morita M, et al: Molecular species of phospholipids with very long chain fatty acids in skin fibroblasts of Zellweger syndrome. *Lipids* 48: 1253−1267, 2013.
15) Yamashita T, Mitsui J, Shimozawa N, Takashima S, Umemura H, et al: Ataxic form of autosomal recessive PEX10-related peroxisome biogenesis disorders with a novel compound heterozygous gene mutation and characteristic clinical phenotype. *J Neurol Sci* 375: 424−429, 2017.
16) Thomas MC, Mitchell TW, Harman DG, Deeley JM, Murphy RC, et al: Elucidation of double bond position in

unsaturated lipids by ozone electrospray ionization mass spectrometry. *Anal Chem* 79: 5013−5022, 2007.

17) Moe MK, Anderssen T, Strøm MB, Jensen E: Total structure characterization of unsaturated acidic phospholipids provided by vicinal di-hydroxylation of fatty acid double bonds and negative electrospray ionization mass spectrometry. *J Am Soc Mass Spectrom* 16: 46−59, 2005.

18) Bollinger JG, Thompson W, Lai Y, Oslund RC, Hallstrand TS, et al: Improved sensitivity mass spectrometric detection of eicosanoids by charge reversal derivatization. *Anal Chem* 82: 6790−6796, 2010.

19) Zhao Y, Zhao H, Zhao X, Jia J, Ma Q, et al: Identification and quantitation of C=C location isomers of unsaturated fatty acids by epoxidation reaction and tandem mass spectrometry. *Anal Chem* 89: 10270−10278, 2017.

20) Wang M, Han RH, Han X: Fatty acidomics: Global analysis of lipid species containing a carboxyl group with a charge-remote fragmentation-assisted approach. *Anal Chem* 85: 9312−9320, 2013.

21) Moser HW, Moser AB, Frayer KK, Chen W, Schulman JD, et al: Adrenoleukodystrophy: Increased plasma content of saturated very long chain fatty acids. *Neurology* 31: 1241−1249, 1981.